过去 6.0 ~2.0 Ma 大气铁载荷及其指示的北半球大冰期发生的可能原因

曹军骥,安芷生
(中国科学院地球环境研究所 黄土与第四纪地质国家重点实验室,西安 710075)

摘 要:基于中国中部的一个沉积序列的铝浓度重建了过去 6.0 ~2.0 Ma 的大气铁载荷与粉尘通量变化。铁载荷从 6.0 Ma 的 ~0.3 μg·m^{-3} 开始增加,到 3.0 Ma 左右达到最高值约 1.2 μg·m^{-3},然后开始迅速下降。黄土高原的大气铁载荷和粉尘通量变化型式与 ODP 885/886 孔的粉尘通量,以及 ODP 882 孔的生物蛋白石海洋沉积速率的变化型式一致,都显示了从 6.0 Ma 到 2.7 Ma 的增加趋势。这表明粉尘的海气交换最可能通过铁肥机制影响海洋生产力。从 3.6 Ma 至2.7 Ma,铁载荷与北太平洋古海洋生产力及全球大气 CO_2 的变化存在高度一致性,指示了粉尘/铁通量的增加及其导致的各种反馈作用很可能加速北半球大冰期的发生。

关键词:大气铁载荷;粉尘通量;古海洋生产力;大气 CO_2
中图分类号: P461; P402 **文献标志码**: A **文章编号**:1674-9901(2010)01-0052-08

Atmospheric iron loading in Asia during 6.0 ~2.0 Ma and implications for the onset of Northern Hemisphere Glaciation

CAO Jun-ji, AN Zhi-sheng
(State Key Laboratory of Loess and Quaternary Geology, Institute of Earth Environment, Chinese Academy of Sciences, Xi'an 710075, China)

Abstract: Atmospheric iron loadings and dust fluxes for the last 6.0 to 2.0 Ma before the present were reconstructed from Al concentrations in a sediment profile from central China. Iron loadings increased from ~0.3 μg·m^{-3} at 6.0 Ma and peaked at ~1.2 μg·m^{-3} around 3.0 Ma then decreased sharply. The patterns of atmospheric Fe loadings and dust fluxes to the loess plateau, the dust fluxes at ODP site 885/886, and the marine accumulation rate of biogenic opal at the ODP site 882 all show similar increasing trends from 6.0 to 2.7 Ma. This suggests that the air/sea exchange of dust influenced marine productivity, most likely through an iron-fertilization mechanism. A strong coherence between the evolution of iron loadings with the variations of paleoproductivity in North Pacific and global atmospheric CO_2 was found from 3.6 to 2.7 Ma, this implies that increased dust/iron fluxes and associated feedbacks may have accelerated the onset of glaciation in the Northern Hemisphere.

Key words: atmospheric iron loading; dust flux; ocean paleoproductivity; atmospheric CO_2

1 Introduction

Increases in atmospheric dust loads have been recognized as one of the factors that may have contributed to the initiation of Northern Hemisphere Glaciation (NHG) (Rea et al, 1998; An et al, 2001). Rea et al (1998) showed the eolian dust accumulation at the Ocean Drilling Program (ODP) site 885/886 in the central North Pacific increased by an order-of-magnitude over a short time period

Received date: 2010-05-07
Foundation item: National Basic Research Program of China (2010CB833400)
Corresponding author: CAO Jun-ji, E-mail: cao@ loess. llqg. ac. cn

beginning around 3.6 Ma before the present (BP). This increased dust flux was linked to a 1-Ma-long shift toward heavy $\delta^{18}O$ values, which indicated that a cooling period occurred between 3.6 and 2.6 Ma. In addition to the direct radiative effects of dust, as implicated by Rea et al (1998), the air/sea exchange of eolian iron connects oceanic biogeochemistry with the Earth's climate system (Jickells et al, 2005). That is, increased dust/iron concentrations in the atmosphere and higher rates of iron deposition into the oceans could enhance primary productivity in the ocean, and this in turn could enhance the drawdown of atmospheric CO_2 by the ocean, thus cooling the Earth's surface (Martin, 1990).

This "Iron Hypothesis" has been invoked to explain variations in glacial-interglacial atmospheric CO_2 through the control of paleoproductivity during the late Quaternary (Martin, 1990). The deposition of nutrient iron provides a plausible paradigm for the global modification of the ocean's productivity over geological time scales; however, the connections between dust and ocean productivity in Asia-Pacific regions and their roles in global climatic systems in the long-term geological evolution remain unclear. Here we recover the high-resolution variations of atmospheric iron loadings and dust fluxes from 6.0 to 2.0 Ma from red clay deposits in central China. These reconstructed loadings are an important tool for investigating climate change because they can be directly compared with present-day observations. Examination of the coupled evolution of dust/iron and paleoprodutivity-CO_2 in the Asia-Pacific region provides a means for evaluating the dust/iron connections to the climatic system.

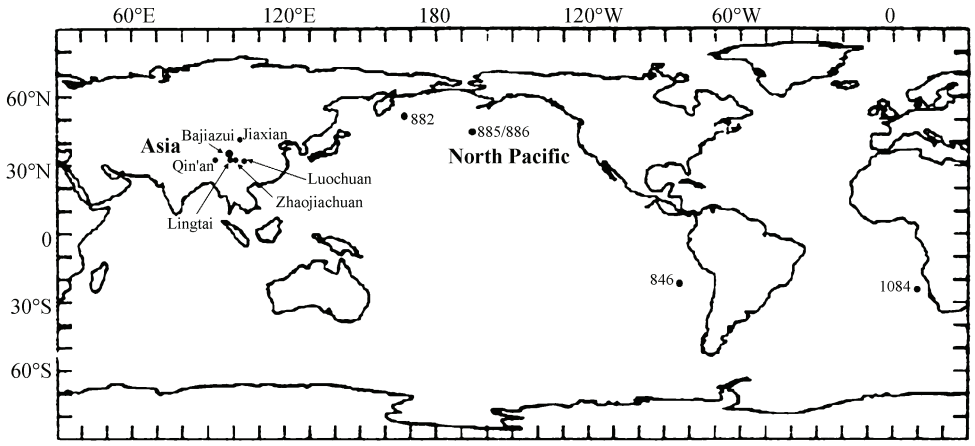

Fig. 1 The locations of continental and marine sites

2 Methods

The wind-blown red-clay sequences in central China are arguably the most complete records of Asian dust, covering at least 6 Ma BP (Sun et al, 1997; An et al, 2001; Qiang et al, 2001; Guo et al, 2002; Xu et al, 2009). These red-clays were deposited quickly and changed little during loessification; this makes them nearly ideal for reconstructing high-resolution dust records. The classic Bajiazui loess section (35°53′N, 107°27′E, Fig. 1) was selected for our study to recover dust fluxes and atmospheric iron loadings over Asia from 6.0 to 2.0 Ma. This profile is overlaid by a Quaternary loess-palaeosol sequence and lies over a base of late Tertiary fluvial fine-sand. Its thickness is about 66 m with light-reddish areas that have experienced only weak pedogenesis. Detailed geological descriptions and a stratigraphic framework for the sequence have been provided by Sun et al (1997) and An et al (2001).

A total of 645 samples was taken at intervals of 10 cm for Al and Fe elemental analysis. The samples were digested with a mixture of strong acids (HF, $HClO_4$, and HNO_3), and the analyses were carried out with the use of an inductively coupled plasma-mass spectrometer (ICP-MS, SOLA, Finnigan UK), which has a precision (i.e., relative standard deviation) of about 10%. In addition, 64 samples were taken at intervals of 1 m for grain size analysis; these were done by laser diffraction using a Mastersizer (MS 2000,

Malvern UK).

Elemental Al fluxes (F_{Al}) were reconstructed using the Al flux methodology of Zhang et al (1994):

$$F_{Al} = C_{Al}\rho\ LDR \quad (1)$$

where C_{Al} refers to the concentration of aluminum in each red clay sample, ρ is the bulk density of dust particles (2.5 g · cm^{-3}, Giorgi, 1988), and LDR is the linear deposition rate of red clay material.

The dust fluxes (F_{dust}), in turn, were calculated from the aluminum fluxes, assuming 7% Al by weight for Asian dust (Zhang et al, 2003).

$$F_{dust} = F_{Al}/7\% \quad (2)$$

Past atmospheric dust loadings (C_{dust}) were reconstructed from the dust fluxes and estimates of deposition velocities (V_{dust}) extracted from red clay records:

$$C_{dust} = F_{dust}/V_{dust} \quad (3)$$

Here the dry deposition velocity methodology of Zhang et al (2002) was used to back calculate V_{dust}; that is:

$$V_{dust} = 0.235 \times D_{99\%} - 3.65 \quad (4)$$

where $D_{99\%}$ refers to the particle diameter corresponding to the uppermost 1% of the cumulative mass distribution, which is estimated from measured red-clay particle-size distributions.

Atmospheric iron loadings were calculated by converting the dust concentrations into iron based on the observed percentage of iron in the red clay (P_{iron}); thus:

$$C_{iron} = C_{dust} \times P_{iron} \quad (5)$$

3 Results and Discussion

3.1 Trends in the dust and iron concentrations and fluxes

Variations in atmospheric iron loadings from 6.0 ~ 2.5 Ma as reconstructed from the Bajiazui profile in central China are illustrated in Fig. 2a. Prior to 4.2 Ma, the iron loadings fluctuated from approximately 0.1 μg · m^{-3} ~ 0.4 μg · m^{-3} (Table 1), and then from 4.2 ~3.6 Ma, eolian Fe increased from ~0.2 ~0.8 μg · m^{-3}. From 3.6 ~2.7 Ma, the Fe loadings rose quickly, with the highest values reaching 1.2 μg · m^{-3}. After 2.7 Ma, atmospheric Fe decreased from ~ 0.9 μg · m^{-3} ~0.2 μg · m^{-3}. For the most part, dust fluxes share a similar pattern with iron loadings, but they exhibit different trends after 2.7 Ma (Fig. 2a). That is, the dust fluxes increased after 2.7 Ma while atmospheric Fe decreased; this is due to differences in elemental composition as a function of particle-size in the red clays.

Table 1 Iron loading, dust loading, and dust flux reconstructed from the Bajiazui profile compared with other studies

Quantity	Site	Unit	Time Period				
			6.0 ~4.2 Ma	4.2 ~3.6 Ma	3.6 ~2.7 Ma	2.7 ~2.5 Ma	
Iron loading	Bajiazui	μg · m^{-3}	0.25 (0.11 ~0.42)	0.43 (0.19 ~0.78)	0.67 (0.3 ~1.15)	0.58 (0.23 ~0.93)	
	Central China	μg · m^{-3}					7 ~28[a]
Dust Loading	Bajiazui	μg · m^{-3}	5.1 (2.8 ~7.9)	7.7 (4.0 ~12.1)	12.0 (5.3 ~22.8)	12.9 (7.4 ~18.3)	
	Luochuan	μg · m^{-3}					41 ~171[b]
Dust Flux	Bajiazui	g · m^{-2} · a^{-1}	2.0 (1.0 ~3.3)	2.8 (1.5 ~4.8)	4.2 (1.9 ~8.0)	6.1 (3.7 ~9.9)[c]	
	Luochuan[2]	g · m^{-2} · a^{-1}					9 ~41[b]

Notes: a. in the modern atmosphere (Zhang et al, 2003); b. in the last 250 ka (Zhang et al, 2002); c. average time 2.7 to 2.2 Ma

The climate was warm and wet around 5 Ma (Pettke et al, 2000), and those conditions are consistent with the relatively low dust fluxes and iron loadings we found from 5.2 ~ 4.5 Ma. According to Rea et al (1998) the Asian dust source regions began to dry beginning around 4.2 Ma, and at that time the quantities of dust injected into the atmosphere increased. At ~3.6 Ma, the uplift of Tibetan Plateau accelerated, which increased dust concentrations and fluxes (An et al, 2001). From 3.6 ~2.7 Ma, the dust source regions continued to dry and the East Asia winter monsoon strengthened, these two factors favoured further increases in dust production (An et al, 2001) (Fig. 2a、2b). The reconstructed dust fluxes from our site and sedimentation at ODP site 885/886 show generally similar patterns from 6.0 to 2.0 Ma. The eolian depositional fluxes recorded in both of these environments were relatively low before the drying period that began around 4.2 Ma, then they both apparently increased, with sharper increases after

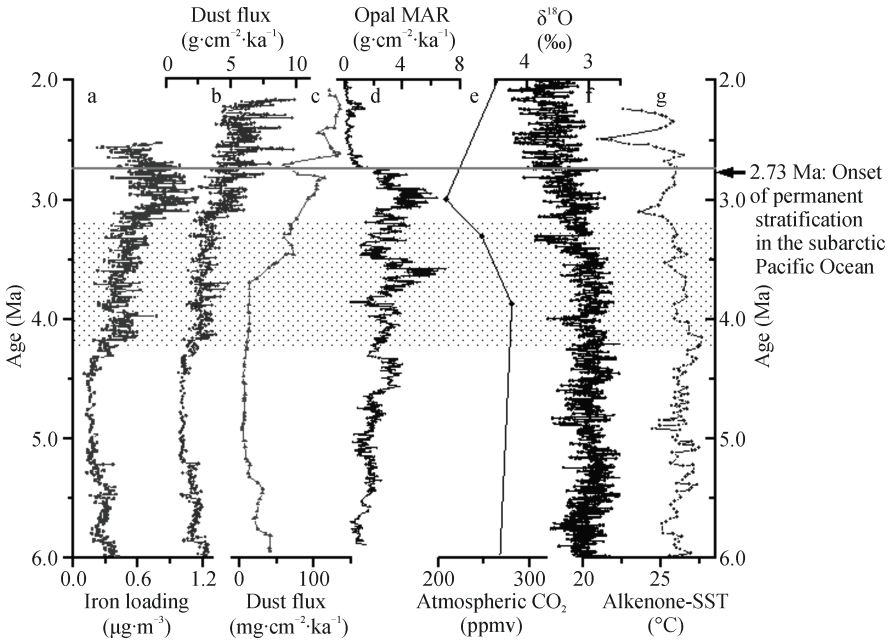

Fig. 2 Time series plots of atmospheric Fe loading, dust flux, biogenic opal MAR, atmospheric CO_2, ice volume and sea surface temperatures (SST) from 6.0 to 2.0 Ma before the present. Shading highlights the period from 4.2 to 2.73 Ma and yellow shading highlights 3.2 to 2.73 Ma Grey line at 2.73 Ma marks the onset of permanent stratification in the subarctic Pacific Ocean. a. The atmospheric Fe loading reconstructed from the Bajiazui profile (the Fe loading was lacked during 2 ~ 2.5 Ma since the absence of grain size analysis); b. Dust flux recorded in the Bajiazui profile; c. Dust flux at OPD site 885/886 (Rea et al, 1998); d. Biogenic Opal MAR at OPD site 882 (Haug et al, 1999); e. Atmospheric CO_2 concentrations (Paul and Palmer, 2000); f. Global ice volume indicated by $\delta^{18}O$ from ODP 846 (Shackleton et al, 1995); g. Alkenone-based sea surface temperature (SST) recorded at ODP site 1084 (Marlow et al, 2000).

3.6 Ma. The dust flux after 4.2 Ma was about twice the prior values for the continental sediments (Fig. 2b), and for the marine sediments the later values were ~10-fold larger (Fig. 2c). To evaluate changes in the dust and iron concentrations and fluxes over time, arithmetic mean values were calculated and compared for different time intervals. The results summarized in Table 1 show that the average iron concentration increased from 0.25 $\mu g \cdot m^{-3}$ from 6.0 to 4.2 Ma to 0.43 $\mu g \cdot m^{-3}$ from 4.2 to 3.6 Ma. The highest Fe loading (0.67 $\mu g \cdot m^{-3}$) occurred between 3.6 to 2.7 Ma and then decreased to 0.58 $\mu g \cdot m^{-3}$ from 2.7 to 2.5 Ma (Table 1). The reconstructed iron loading from 6.0 to 2.5 Ma was less than one-tenth of that observed in the contemporary atmosphere of central China (7 to 28 $\mu g \cdot m^{-3}$, Zhang et al, 2003).

The highest average atmospheric dust load (12.9 $\mu g \cdot m^{-3}$) was calculated for the interval between 2.7 to 2.5 Ma; this is between 10% to 40% of the values estimated for the glacial-interglacial atmosphere of Luochuan (35°45′N, 109°25′E, Zhang et al, 2002) (Fig. 1). Average values for the dust fluxes follow the same trends as those of the dust loadings, and these fluxes are 2-fold to 5-fold lower than those at the Luochuan section (Zhang et al, 2002, Table 1). These comparisons indicate that the atmosphere over central Asia from 6.0 to 2.0 Ma was much less dusty compared with glacial-interglacial or present-day conditions.

3.2 Relationships between eolian iron, biological productivity in the oceans, and climate

Dust emissions from central Asia have been ranked as the second largest source of dust on a global scale (Duce et al, 1995), and the long-range transport of Asian dust to the remote North Pacific and as far as North America is now well documented. The transport of aeolian dust from central Asia began at least 22 Ma (Guo et al, 2002), and around 6 to 8 Ma ago, large quantities of Asian dust began to be produced, transported and deposited; these processes

led to the formation of the expansive loess deposits of central China (Sun et al, 1998; An et al, 2001; Qiang et al, 2001; Xu et al, 2009). Mineralogical, geochemical and sedimentological analyses have established that arid lands in central Asia also are the main source for deep-sea sediments of the North Pacific (Rea et al, 1998; Petit et al, 1999).

A high-resolution record of the biogenic opal mass accumulation rate (MAR, Fig. 2d) recovered from ODP site 882 (Fig. 1) was used as an indicator of paleoproductivity in the Subarctic Pacific (Haug et al, 1999), and it serves as a basis for comparisons with our reconstructed Fe data. The iron loadings and opal MAR patterns co-vary over time, especially from 3.6 Ma to 2.7 Ma (Fig. 2), e. g., their values increased from 3.6 to 3.0 Ma, and then both dropped at about the same time. The opal MAR and iron loadings both show increasing trends prior to 2.7 Ma; the opal MAR increased from ~ 1.5 $g \cdot cm^{-2} \cdot ka^{-1}$ at 5.8 Ma to 3.5 $g \cdot cm^{-2} \cdot ka^{-1}$ at 4.5 Ma, then decreased to 2 $g \cdot cm^{-2} \cdot ka^{-1}$ at 4.2 Ma before increasing again to 5.5 $g \cdot cm^{-2} \cdot ka^{-1}$ around 3.0 Ma. After 3.0 Ma, the opal MAR decreased to ~ 2.0 $g \cdot cm^{-2} \cdot ka^{-1}$ at 2.7 Ma and then dropped sharply to 0.3 $g \cdot cm^{-2} \cdot kyr^{-1}$, ostensibly due to the onset of permanent stratification in the Subarctic Pacific Ocean (Haug et al, 1999).

Correlation coefficients (r) between iron loadings and opal MAR were 0.29 for 2.53 to 2.73 Ma, 0.42 for 2.73 to 3.6 Ma, and 0.32 for 3.6 to 6.0 Ma. The highest correlation coefficient for 2.73 to 3.6 Ma (r = 0.42) was statistically significant at a probability for chance occurrence of $p < 5\%$, and this is indicative of stronger connections between iron inputs and biological productivity during that period. Biogenic silica contents from site 885/886 also indicated that the peak paleoproductivity in the Subarctic Pacific occurred at ~3.0 Ma (Dickens and Owen, 1996). The diatom MAR at site 438 off northeast Japan showed that paleoproductivity reached its highest value (4 $g \cdot cm^{-2} \cdot ka^{-1}$) from 3.1 to 2.7 Ma (Barron, 1998). Therefore, a variety of records attest to relatively high levels of paleoproductivity over a broad expanse of the North Pacific at ~3 Ma.

Parts of the North Pacific, especially the Subarctic Pacific, have been classified as "high nitrate (or high nutrient) low chlorophyll" (HNLC) regions (Haug et al, 1999; Kawahata et al, 2000). That is, the phytoplankton standing stocks in these waters are relatively low despite the availability of nitrate and other nutrients (phosphate and silicate) that under other circumstances typically limit biological production. Iron has been proposed as a limiting nutrient in HNLC regions (Martin, 1990; Coale et al, 1996), and under these conditions it is the limited supply of iron that prevents the so-called "biological pump" from working at its maximum efficiency (i.e., completely using all of the available NO_3^-). Close relationships between air/sea exchange of eolian dust and biological production have been reported from field observations (Young et al, 1991; Bishop et al, 2002; Yuan and Zhang, 2006), iron enrichment experiments (Tsuda et al, 2003; Turner et al, 2004), and the analyses of geological records (Kawahata et al, 2000).

An increased quantity of dust in the atmosphere implies greater inputs of iron into the ocean, and for iron-limited phytoplankton communities, nitrogen fixation would likely increase (Orcutt et al, 2001) and a greater proportion of the available major nutrients would be consumed. Previously, Berger and Wefer (1991) speculated that dust from the Asian deserts may have stimulated the productivity of coccolithophores in the northern Pacific in the late Miocene. Indeed, there is a strong analogy between the modern oceanic conditions and those of Subarctic Pacific after the late Miocene (about 6 Ma, Barron, 1998; Haug et al, 1999). Furthermore, a connection between Asian dust/iron inputs and paleoproductivity has been invoked to explain the patterns in carbon isotope records from the late Miocene (~7.6 to 6.6 Ma) and marine biological productivity at ODP site 846 in the Eastern Pacific (Fig. 1) (Diester-Haass et al, 2006).

The biogeochemical response of the oceans to enhanced iron inputs can be envisioned as a priming of the biological pump, and this in turn may lead to feedbacks between the atmosphere and climate systems. For example, increased primary production

would lead to the drawdown of CO_2 and also would affect the air/sea exchange of radiatively-active trace gases and aerosol particles (Charlson et al, 1987; Falkowski, 1998; Jickells et al, 2005). Current models predict that glacial/interglacial changes in dust fluxes would change atmospheric pCO_2 by less than 30 parts per million (10^{-6}); this is roughly a third of the total estimated change of 80×10^{-6} to 100×10^{-6} (Bopp et al, 2003), and thus other forces also were at work; these are discussed briefly below.

Atmospheric CO_2 exhibited a minimum at around 3.0 Ma (Fig. 2e), and one explanation for this is that an increase in phytoplankton abundances led to the drawdown of CO_2. Sigman et al (2004) suggested that an increase in the dust/iron input affected the utilization of nitrate in the Subarctic Pacific around 2.7 Ma, and as noted above Haug et al (1999) linked the opal MAR to stratification of the polar ocean. Therefore, both an increase in the supply of eolian iron and changes in the oceanic circulation may have contributed to the increased opal MAR and the decrease in CO_2. Yet another hypothesis concerning the lowering of CO_2 at 3.0 Ma is that chemical weathering of the Tibetan mountains consumed some of the atmospheric CO_2 (Raymo, 1997).

The trends in atmospheric Fe loadings and dust fluxes to the Loess Plateau, the dust fluxes at ODP site 885, and the biogenic opal MAR at ODP site 882 all show similar increasing trends from 6.0 to 2.7 Ma. Coincident increases are also observed between dust production in Asia (Fig. 2a、2b) and ocean paleoproductivity in the Pacific (Fig. 2d) starting around 4.2 Ma. These occur at the same time as gradual decreases were observed in CO_2, global ice volume (Fig. 2f) and sea surface temperature (SST, Fig. 2g). From 3.2 Ma to 2.7 Ma, the atmospheric Fe loading to the loess Plateau, dust flux at ODP 885 and biogenic opal MAR covary, increasing and decreasing simultaneously. In contrast, variations in atmospheric CO_2 and SST follow opposite trends, e.g., CO_2 reached its minimum value and the SST dropped to about 5℃ at around 3.0 Ma. After 2.73 Ma, the oceanic productivity does not appear to respond to the increased dust supply, and this can be explained by the aforementioned stratification of the subarctic Pacific (Haug et al, 1999).

The coupled evolution of dust, paleoproductivity and CO_2 implies dynamic links amongst them, and here we present a brief narrative of how the connections involving eolian iron, biological production, and climate may have functioned in the Asia/Pacific region. Beginning around 6 Ma, dust emissions from central Asia began to increase due to drier conditions on the continent, and more dust was transported to the North Pacific as the westerly winds also increased in strength (Rea et al, 1998). From 3.6 to 2.6 Ma, the dust concentrations increased and the dusts' transport pathways were affected by the uplift of the Tibetan Plateau (Rea et al, 1998; An et al, 2001). The increased supply of dust/iron eased the iron limitation in the open waters of the North Pacific, which promoted the growth of plankton populations (Jickells et al, 2005) and also stimulated N_2 fixation (Falkowski, 1997; Orcutt et al, 2001). The operation of the biological pump increased with the greater iron flux, and as more atmospheric CO_2 was sequestrated in the ocean, the climate cooled.

These relationships can be envisioned as follows: increased atmospheric iron loadings and fluxes → increased marine productivity → lower CO_2 → colder climate (Jickells et al, 2005). Furthermore, feedbacks may have arisen as the large-scale cooling (indicated by the increase in global ice volume, Fig. 2f), resulted in the growth of arid lands. The larger source areas for dust caused the mineral aerosol loadings over Asia to increase still further (Fig. 2a ~ 2c), and the deposition of the dust from the expanded deserts formed the red clay deposits in China (e.g., Lingtai section in Sun et al, 1998; Jiaxia section in Qiang et al, 2001; Zhaojiachuan section in An et al, 2001; Qin'an section in Guo et al, 2002; Shilou section in Xu et al, 2009) (Fig. 1).

Positive feedbacks between atmospheric dust loads, CO_2 and large-scale cooling (Ridgwell, 2002) may thus have contributed to the development or the intensification of the Northern Hemisphere Glacitation (NHG) (An et al, 2001; Mudelsee and Raymo, 2005). Tectonic forcing, especially the closing of the

Panama Seaway and the uplift of the Tibetan plateau, has been invoked as the likely root cause of the NHG (Mudelsee and Raymo, 2005), but several other factors, such as the Milankovitch orbital motions, changes in oceanic circulation, and changes in sea-ice occurrence, are thought to have been involved (Rea et al, 1998; Hay et al, 2002; Mudelsee and Raymo, 2005; Reynolds et al, 2008). Our studies suggest that the increased dust/iron loadings that accompanied the Tibetan uplift may have further contributed to global cooling due to both short-term radiative effects (Rea et al, 1998; Arimoto, 2001) and longer-term biogeochemical feedbacks (Jickells et al, 2005).

4 Conclusions

Reconstructed records of the atmospheric Fe loadings, the dust fluxes to the Loess Plateau and the biogenic opal MAR at site 882 all show similar increasing trends from 6.0 to 2.7 Ma. These similar trends are further evidence that the air/sea exchange of eolian iron transported from arid lands in central Asia may have a significant impact on marine productivity in the North Pacific. Furthermore, the similar trends in reconstructed iron loadings, paleoproductivity at ODP site 882, and atmospheric CO_2 from 3.6 to 2.7 Ma imply that increased dust/iron and its induced feedbacks may have contributed to the onset of Northern Hemisphere Glaciation. While we have presented evidence that the iron-connection mechanism was operating in Asia-Pacific region from 6.0 to 2.7 Ma, especially from 3.6 to 2.7 Ma, further investigations and modelling studies are needed to fully understand the controls acting on the Earth's climate. This natural fertilization of North Pacific region by eolian iron from arid lands in Asian has occurred over the last several million years. In a more modern context, a better understanding of the mechanisms and processes involved may provide a framework for developing large-scale engineering efforts to combat global climate change, such as the fertilization of the oceans with iron as a means of sequestering anthropogenic carbon.

Acknowledgements: We thank Dr. G. H. Haug from Geoforschungszentrum Potsdam, Germany for providing the paleoproductivity data for ODP site 882.

References:

An Z S, Kutzbach J E, Prell W L, et al. 2001. Evolution of Asian monsoons and phased uplift of the Himalaya – Tibetan plateau since Late Miocene times [J]. *Nature*, 411:62-66.

Arimoto R. 2001. Eolian dust and climate:relationships to sources, tropospheric chemistry, transport and deposition [J]. *Earth-Science Reviews*, 54:29-42.

Barron J A. 1998. Late Neogene changes in diatom sedimentation in the North Pacific [J]. *Journal of Asian Earth Sciences*, 16:85-95.

Berger W H, Wefer G. 1991. Productivity of the glacial ocean: discussion of the iron hypothesis [J]. *Limnology and Oceanography*, 36:1899-1918.

Bishop J K B, Davis R E, Sherman J T. 2002. Robotic observations of dust storm enhancement of carbon biomass in the North Pacific [J]. *Science*, 298:817-820.

Bopp L, Kohfeld K E, Quere C L, et al. 2003. Dust impact on marine biota and atmospheric CO_2 during glacial periods [J]. *Paleoceanography*, 18(2):1046, doi:10.1029/2002PA000810.

Charlson R J, Lovelock J E, Andreae M O, et al. 1987. Oceanic phytoplankton, atmospheric sulphur, cloud albedo and climate [J]. *Nature*, 326:655-661.

Coale K, Johnson K S, Fitzwater S E, et al. 1996. A massive phytoplankton bloom induced by an ecosystem-scale iron fertilization experiment in the equatorial Pacific Ocean [J]. *Nature*, 383:495-501.

Dickens G R, Owen R M. 1996. Sediment geochemical evidence for an early-middle Gilbert (early Pliocene) productivity peak in the North Pacific Red Clay Province [J]. *Marine Micropaleontology*, 27:107-120.

Diester-Haass L, Billups K, Emeis K C. 2006. Late Miocene carbon isotope records and marine biological productivity: Was there a (dusty) link? [J]. *Paleoceanography*, 21: PA4216, doi:10.1029/2006PA001267.

Duce R A. 1995. Sources, distributions, and fluxes of mineral aerosols and their relationship to climate[M]//Charlson, R J, Heintzenberg J. Aerosol Forcing of Climate. New York:Wiley,43-72.

Falkowski P G, Barber R T, Smetacek V. 1998. Biogeochemical controls and feedbacks on ocean primary production [J]. *Science*, 281:200-206.

Falkowski P G. 1997. Evolution of the nitrogen cycle and its influence on the biological sequestration of CO_2 in the ocean[J]. *Nature*, 387:272-275.

Giorgi F. 1988. Dry deposition velocities of atmospheric aerosols as inferred by applying a particle dry deposition

parameterization to a general circulation model [J]. *Tellus*, 40B:23-41.

Guo Z T, Ruddiman W F, Hao Q Z, et al. 2002. Onset of Asian desertification by 22 Myr ago inferred from loess deposits in China [J]. *Nature*, 416:159-163.

Haug G H, Sigman D M, Tiedemann R, et al. 1999. Onset of permanent stratification in the subarctic Pacific Ocean [J]. *Nature*, 401:779-782.

Hay W W, Soeding E, DeConto R M, et al. 2002. The Late Cenozoic uplift - climate change paradox [J]. *Int J Earth Sci (Geol Rundsch)*, 91:746-774.

Jickells T D, An Z S, Andersen K K, et al. 2005. Global iron connections between desert dust, ocean biogeochemistry, and climate [J]. *Science*, 308:67-71.

Kawahata H, Okamoto T, Matsumoto E, et al. 2000. Fluctuations of eolian flux and ocean productivity in the mid-latitude North Pacific during the last 200 kyr [J]. *Quat Sci Rev*, 9:1279-1282.

Marlow J R, Lange C B, Wefer G, et al. 2000. Upwelling intensification as part of the Pliocene-Pleistocene climate transition [J]. *Science*, 290:2288-2291.

Martin J H. 1990. Glacial-interglacial CO_2 change: the Iron hypothesis[J]. *Paleoceanography*, 5:1-13.

Mudelsee M, Raymo M E. 2005. Slow dynamics of the Northern Hemisphere glaciation [J]. *Paleoceanography*, 20, PA4022, doi:10.1029/2005PA001153, 2005.

Orcutt K M, Lipschultz F, Gundersen K, et al. 2001. Seasonal pattern and significance of N_2 fixation by Trichodesmium spp. at the Bermuda Atlantic Time-series Study (BATS) site [J]. *Deep-Sea Research II*, 48:1683-1608.

Paul N P, Palmer M R. 2000. Atmospheric carbon dioxide concentrations over the past 60 million years [J]. *Nature*, 406:695-699.

Pettke T, Halliday A N, Hall C M, et al. 2000. Dust production and deposition in Asia and the north Pacific Ocean over the past 12 Myr [J]. *Earth Planet Sci Lett*, 178:397-413.

Qiang X K, Li Z X, Powell C McA, et al. 2001. Magnetostratigraphic record of the Late Miocene onset of the East Asian monsoon, and Pliocene uplift of northern Tibet [J]. *Earth Planet Sci Lett*, 187:83-93.

Raymo M. 1997. Carbon cycle models: how strong are the constraints?[M] // Ruddiman W F. Tectonic uplift and climate change. New York: Plenum Press, 367-381.

Rea D K, Snoeckx H, Joseph L H. 1998. Late Cenozoic eolian deposition in the North Pacific: Asian drying, Tibetan uplift, and cooling of the northern hemisphere [J]. *Paleoceanography*, 13:215-224.

Reynolds B C, Frank M, Halliday A N. 2008. Evidence for a major change in silicon cycling in the subarctic North Pacific at 2.73 Ma [J]. *Paleoceanography*, 23, PA4219, doi:10.1029/2007PA001563.

Ridgwell A J. 2002. Dust in the Earth system: the biogeochemical linking of land, air and sea [J]. *Phil Trans R Soc Lond A*, 360:2905-2924.

Shackleton N J, Hall M A, Pate D. 1995. Pliocene stable isotope stratigraphy of site 846 [J]. *Proc ODP Sci Res*, 138:337-355.

Sigman D M, Jaccard S L, Haug G H. 2004. Polar ocean stratification in a cold climate [J]. *Nature*, 428:59-63.

Sun D H, Liu D S, Chen M Y, et al. 1997. Magnetostratigraphy and palaeoclimate of red clay sequences form Chinese Loess Plateau [J]. *Science in China (Series, D)*, 40:337-343.

Sun D H, Shaw J, An Z S, et al. 1998. Magnetostratigraphy and paleoclimatic interpretation of a continuous 7.2 Ma Late Cenozoic eolian sediments from the Chinese Loess Plateau [J]. *Geophys Res Lett*, 25:85-88.

Tsuda A, Takeda S, Saito H, et al. 2003. A mesoscale iron enrichment in the Western Subarctic Pacific induces a large centric diatom bloom [J]. *Science*, 300:958-961.

Turner S M, Harvey M J, Law C S, et al. 2004. Iron-induced changes in oceanic sulfur biogeochemistry [J]. *Geophys Res Lett*, 31:L14307, doi:10.1029/2004GL020296.

Xu Y, Yue L P, Li J X, et al. 2009. An 11-Ma-old red clay sequence on the Eastern Chinese Loess Plateau [J]. *Palaeogeography, Palaeoclimatology, Palaeoecology*, 284: 383-391.

Young R W, Carder K L, Betzer P R, et al. 1991. Atmospheric iron input and primary productivity: phytoplankton responses in the north Pacific [J]. *Global biogeochem cycles*, 5:119-134.

Yuan W, Zhang J. 2006. High correlations between Asian dust events and biological productivity in the western North Pacific[J]. *Geophys Res Lett*, 33, L07603, doi:10.1029/2005GL025174.

Zhang X Y, An Z S, Chen T, et al. 1994. Late quaternary records of the atmospheric input of eolian dust to the center of the Chinese Loess Plateau [J]. *Quat Res*, 41: 35-43.

Zhang X Y, Gong S L, Arimoto R, et al. 2003. Characterization and Temporal Variation of Asian Dust Aerosol from a Site in the Northern Chinese Deserts [J]. *J Atmos Chem*, 44:241-257.

Zhang X Y, Lu H Y, Arimoto R, et al. 2002. Atmospheric dust loadings and their relationship to rapid oscillations of the Asian winter monsoon climate: two 250-kyr loess records[J]. *Earth Planet Sci Lett*, 202:637-643.